Development 134, 3917-3928 (2007) doi:10.1242/dev.008441

HIF1α regulation of *Sox9* is necessary to maintain differentiation of hypoxic prechondrogenic cells during early skeletogenesis

Roy Amarilio[1], Sergey V. Viukov[1], Amnon Sharir[1], Idit Eshkar-Oren[1], Randall S. Johnson[2] and Elazar Zelzer[1,*]

During early stages of limb development, the vasculature is subjected to extensive remodeling that leaves the prechondrogenic condensation avascular and, as we demonstrate hereafter, hypoxic. Numerous studies on a variety of cell types have reported that hypoxia has an inhibitory effect on cell differentiation. In order to investigate the mechanism that supports chondrocyte differentiation under hypoxic conditions, we inactivated the transcription factor hypoxia-inducible factor 1α (HIF1α) in mouse limb bud mesenchyme. Developmental analysis of *Hif1α*-depleted limbs revealed abnormal cartilage and joint formation in the autopod, suggesting that HIF1α is part of a mechanism that regulates the differentiation of hypoxic prechondrogenic cells. Dramatically reduced cartilage formation in *Hif1α*-depleted micromass culture cells under hypoxia provided further support for the regulatory role of HIF1α in chondrogenesis. Reduced expression of *Sox9*, a key regulator of chondrocyte differentiation, followed by reduction of *Sox6*, collagen type II and aggrecan in *Hif1α*-depleted limbs raised the possibility that HIF1α regulation of *Sox9* is necessary under hypoxic conditions for differentiation of prechondrogenic cells to chondrocytes. To study this possibility, we targeted *Hif1α* expression in micromass cultures. Under hypoxic conditions, *Sox9* expression was increased twofold relative to its expression in normoxic condition; this increment was lost in the *Hif1α*-depleted cells. Chromatin immunoprecipitation demonstrated direct binding of HIF1α to the *Sox9* promoter, thus supporting direct regulation of HIF1α on *Sox9* expression. This work establishes for the first time HIF1α as a key component in the genetic program that regulates chondrogenesis by regulating *Sox9* expression in hypoxic prechondrogenic cells.

KEY WORDS: Hypoxia, HIF1, HIF1α, Mesenchymal condensation, Chondrocyte differentiation, Chondrogenesis, SOX9, Joint formation, Bone development, VEGF, GDF5, BMP, SOX5, SOX6

INTRODUCTION

The formation of the limb skeleton is initiated when pluripotent mesenchymal cells, derived from the lateral plate mesoderm, commit to the chondrogenic lineage and aggregate to form condensations, which, through a series of differentiation steps, form cartilaginous template of the future skeleton.

During the initial stages of this process, the limb vasculature undergoes a remodeling process that renders the condensing mesenchyme avascularized (Feinberg et al., 1986; Hallmann et al., 1987). As the condensations increase in size, cells differentiate into chondrocytes, forming a cartilaginous template of the future bones. The cartilaginous elements of the autopod develop last, as each digit originates from a single condensation known as the digital ray (Oster, 1988). As the digital ray increases in size, it undergoes segmentation, giving rise to the carpal, tarsal and the phalangeal elements. The ensuing formation of joints between the separating segments begins with the appearance of a higher cell density domain, called the interzone, at the site of the future joint. Cells in this region lose typical chondrocyte characteristics, as they reduce the expression of collagen type II (also known as procollagen, type II alpha 1 – Mouse Genome Informatics) and instead express markers such as *Wnt9a*, *Gdf5*, *Bmp2* and noggin (Hartmann and Tabin, 2001; Seemann et al., 2005). Next, the joint cavitates within the interzone, separating the two skeletal elements (Archer et al., 2003; Mitrovic, 1977; Pacifici et al., 2005).

[1]Department of Molecular Genetics, Weizmann Institute of Science, PO Box 26, Rehovot 76100, Israel. [2]Molecular Biology Section, Division of Biology, University of California, San Diego, CA, USA.

*Author for correspondence (e-mail: eli.zelzer@weizmann.ac.il)

Accepted 21 August 2007

As development proceeds, the avascularized cartilaginous template is eroded and replaced by vascularized bone in a process termed endochondral ossification (Karsenty and Wagner, 2002; Kronenberg, 2003; Olsen et al., 2000).

Mesenchymal condensation is the initial step in cartilage formation, and the transcription factor SOX9 is an essential regulator of this process (Bi et al., 1999). Inactivation of *Sox9* in limb mesenchymal and neural crest cells results in complete absence of mesenchymal condensation and subsequent failure in cartilage formation (Akiyama et al., 2002; Mori-Akiyama et al., 2003). Furthermore, SOX9 is needed during the sequential steps that follow mesenchymal condensation. Inactivation of *Sox9* after the condensation step results in chondrodysplasia with severe reduction in cartilage-specific extracellular matrix protein and attenuation in chondrocyte proliferation (Akiyama et al., 2002).

Two other members of the Sox family, namely L-SOX5 and SOX6, are necessary to maintain the chondrocyte differentiation process. Whereas targeting the expression of either *Sox5* or *Sox6* resulted in limited skeletal abnormalities, mutant embryos that lacked both genes showed severe aberrations in cartilage formation (Smits et al., 2001). The precise mechanism that regulates the expression of *Sox9*, *Sox5* and *Sox6* is unknown; nevertheless, normal expression of *Sox9* observed in *Sox5*- and *Sox6*-null mice and the loss of *Sox5* and *Sox6* expression in *Sox9*-deficient mesenchymal cells position *Sox9* upstream from its two family members (Akiyama et al., 2002; Smits et al., 2001).

The regression of blood vessels from sites where mesenchyme condense is likely to induce a localized reduction in oxygen tension at those vessel-free domains, thus forming hypoxic niches. Numerous studies on a variety of cell types have reported that hypoxia has an inhibitory effect on cell differentiation. In view of

that, the expected consequence of hypoxic niche formation at the condensation sites would be differentiation arrest. The implication of mesenchymal differentiation into chondrocytes is the existence of a unique mechanism that enables this process to take place under hypoxic conditions.

The transcription factor complex hypoxia-inducible factor 1 (HIF1) is a key mediator of adaptive responses to changes in cellular oxygen level (Semenza, 1998). HIF1 is a heterodimer that consists of HIF1α, the oxygen sensitive subunit, and the constitutively expressed HIF1β (also referred to as ARNT). Under normoxia, HIF1α is hydroxylated by prolyl hydroxylases that act as oxygen sensors (Semenza, 2004). The hydroxylation of proline residues is followed by rapid proteasomal degradation (Jaakkola et al., 2001). Conversely, when under hypoxic conditions HIF1α is stabilized, as a result of reduced proteasome-mediated degradation. It then binds to HIF1β and enhances the transcription of genes that are involved in glucose metabolism, angiogenesis, and cell survival (Schofield and Ratcliffe, 2004; Semenza, 2003).

A previous study identified HIF1α as a critical factor in chondrocyte survival (Schipani et al., 2001). In that study, *Hif1α* expression was abolished in collagen type II-expressing chondrocytes. Finding that at initial stages of chondrogenesis cells of the forming condensations are hypoxic led us to hypothesize that HIF1α has an additional and yet unidentified role in earlier stages of skeletogenesis.

This study describes a novel role for HIF1α as a regulator of *Sox9* expression in hypoxic prechondrogenic condensations. *Hif1α* deletion in mouse limb mesenchyme led to differentiation arrest of prechondrogenic condensation and resulted in severe skeletal malformations. Moreover, the dramatic reduction in *Sox9* expression in the prechondrogenic condensation, accompanied by misexpression of *Gdf5* and noggin in *Hif1α*-depleted limb, provides a molecular mechanism to explain the joint abnormalities observed in *Hif1α*-depleted limbs. Micromass cultures experiments further supported the role of HIF1α in chondrogenesis: under hypoxic conditions *Sox9* expression increased in control cells; this increment was lost in *Hif1α*-depleted cells. Furthermore, under normoxic conditions *Hif1α* overexpression induced an increase in *Sox9* expression.

Chromatin immunoprecipitation (ChIP) assay provided evidence for direct interaction of HIF1α with the *Sox9* promoter, thus supporting direct regulation of HIF1α on *Sox9* expression. Our findings establish HIF1α as a key component in the mechanism that regulates chondrogenesis by regulating *Sox9* expression in the hypoxic prechondrogenic condensations.

MATERIALS AND METHODS

Animals

The generation of *floxed-Hif1α* (Ryan et al., 2000) and *Prx1* (also known as *Prrx1* – Mouse Genome Informatics)-*Cre* mice (Logan et al., 2002) have been described previously. In all timed pregnancies the day of the vaginal plug appearance was defined as E0.5. For harvesting of embryos, timed-pregnant female mice were sacrificed by CO_2 intoxication. The gravid uterus was dissected out and suspended in a bath of cold PBS, and the embryos were harvested after amnionectomy and removal of the placenta. Tail genomic DNA was used for genotyping.

Skeletal preparations

Cartilage and bones in whole mouse embryos were visualized after staining with Alcian Blue and Alizarin Red S (Sigma) and clarification of soft tissue with potassium hydroxide (McLeod, 1980).

Micro-CT analysis

Three-dimensional high-resolution images were obtained from the left limb of *Prx1-Hif1α* and control embryos using microcomputed tomography (GE Healthcare, London, Ontario, Canada). Scans were taken at 8 μm isotropic resolution. Images were reconstructed and thresholded to distinguish bone voxels with MicroView software version 5.2.2 (GE Healthcare). One threshold was chosen for all specimens.

Histology, immunofluorescence and in situ hybridization

For histology and section in situ hybridization, embryos were fixed overnight in 4% PFA-PBS, dehydrated to 100% ethanol, embedded in paraffin and sectioned at 7 μm. Section and whole-mount in situ hybridizations were performed as described previously (Murtaugh et al., 1999; Riddle et al., 1993). All probes are available on request. Hematoxylin and Eosin (H&E) staining was performed following standard protocols.

For immunofluorescence, embryos were embedded in OCT (Tissue-Tek) and 7 μm cryostat sections were made. Cryosections were fixed for 20 minutes in 4% PFA-PBS, permeabilized with 0.1% Triton X-100 and incubated with anti-CD31 (BD PharMingen), monoclonal anti-HIF1α (Novus Biologicals, Littleton, CO, USA), anti-collagen type II (Developmental Studies Hybridoma Bank, The University of Iowa, IA, USA). Secondary antibodies were purchased from Jackson Laboratories. All experiments were performed with at least three different wild-type (WT) and knockout (KO) limbs from different litters.

Hypoxia detection

Animals were injected with 60 mg/kg hypoxyprobe-1 (Chemicon) and sacrificed 30 minutes after injection. Paraffin sections (7 μm) were stained with FITC-conjugated Hypoxyprobe-1 Mab-1 according to the manufacturer's protocols.

BrdU assay

Female mice were injected with 100 mg/kg BrdU (Sigma) and sacrificed 2 hours later. Embryo limbs were collected, fixed with 4% PFA-PBS, embedded in paraffin and 7 μm sections were made. Further processing was performed with a BrdU staining kit (Zymed). To quantify the rate of cell proliferation, serial images of the same digits were collected and BrdU-positive cells (red) and negative cells (gray) in the phalangeal region were counted in four control and four *Prx1-Hif1α* limbs from two different litters. Statistical significance was determined by Student's *t*-test.

Primary cell culture preparations and viral transfer

For micromass cultures, limbs of E11.0-E11.5 *floxed-Hif1α* embryos were collected, digested with 0.1% collagenase IV, 0.1% trypsin (Sigma) and 2% FCS for 15 minutes. The cell suspension was placed in DMEM-F12, 10% FCS. Cells were plated as 10 μl droplets at 2×10^7 cells/ml. Cells were allowed to attach for 75 minutes and were then overlaid with 300 μl of DMEM-F12, 10% FCS containing 6.5×10^7 viral particles/μl of Adeno-Gfp, Adeno-Cre, Ad-βgal (Gene Transfer Vector Core, University of Iowa) or Adeno-Sox9 (kindly provided by Dr H. Akiyama, Kyoto University, Japan). Medium was changed daily. Cells were cultured either with 20% oxygen (normoxia) or 1% oxygen (hypoxia) balanced with N_2 in a 3-Gas incubator (Heraeus) in a humidified atmosphere. Cells were moved to hypoxia 24 hours after the initial plating, and after 96 hours the cultures were either stained with Alcian Blue (pH 1) to visualize chondrogenic nodule formation or harvested to extract RNA. For lentivirus production, cDNA encoding stabilized human HIF1α was digested from PEF-HIF1α P564A/N803A plasmid (kindly provided by Dr M. Whitelaw, University of Adelaid, South Australia) and subcloned into lentiviral transfer vector (kindly provided by Dr Inder M. Verma, Salk Institute, California). Lentivirus production and purification was carried out according to the method of Tiscornia et al. (Tiscornia et al., 2006).

Immunohistochemistry

For immunohistochemical staining of micromass cultures, cells were fixed for 15 minutes at room temperature with 4% paraformaldehyde in PBS and then washed twice with PBS. Endogenous peroxidase activity was inactivated by incubating the cells for 30 minutes in 1% H_2O_2 in PBS. Cells were subsequently washed three times with PBS, blocked for 30 minutes with PBS, 10% FCS and 0.1% Triton X-100, and incubated with the primary antibodies against collagen type II (II-II6B3 supernatant, 1:30) from the Developmental Hybridoma Bank (Iowa). The signal was detected using a

biotinylated anti-mouse secondary antibody (dilution 1:250; Vector Laboratories) in combination with the ABC Kit (Vector Laboratories) and DAB (Vector Laboratories) as a substrate.

Quantitative RT-PCR

For quantitative RT-PCR analysis, 1 μg total RNA was used to produce first-strand cDNA. Reverse transcription was performed with SuperScriptII (Invitrogen) according to the manufacturer's protocol. Quantitative PCR was performed using SYBR green (Roche). Values were calculated using the second derivative method and normalized to 18S rRNA expression. All primers are available on request.

Western blot analysis

For western blot analysis, protein was extracted from micromass cultures. Protein concentration was determined using the BCA assay (Pierce). SOX9 (1:1000; Santa Cruz Biotechnology) and α-tubulin (1:1000; Sigma) antibodies were used, followed by the appropriate HRP-conjugated secondary antibodies (1:10,000; Jackson ImmunoResearch) and luminol detection.

Chromatin immunoprecipitation

Micromass lysates were prepared as follows: 20 drops, each 10 μl at 2×10^7 cells/ml were plated and either cultured under 1% oxygen (hypoxia) or 20% oxygen (normoxia) for 12 hours. Cells were cross-linked in vivo with 1.5% formaldehyde for 10 minutes in the incubator chamber. The cells were washed once with PBS and incubated with 0.25% trypsin-EDTA for 20 minutes. Cells were washed with 2.5 ml of cold PBS and homogenized in 1 ml of buffer I [10 mM Hepes (pH 6.5), 10 mM EDTA, 0.5 mM EGTA, 0.25% Triton X-100]; lysates were washed once with buffer II [10 mM Hepes (pH 6.5), 1 mM EDTA, 0.5 mM EGTA, 200 mM NaCl]. Cell extracts were prepared for ChIP as described previously (Ainbinder et al., 2004). For immunoprecipitation, 5 μl of either polyclonal anti-HIF1α (Abcam) or control IgG were added to 0.5 ml of the soluble chromatin (corresponding to 5×10^5 cells) and the mixture was incubated overnight at 4°C. Purified DNA from immunoprecipitates, as well as of the input material, was analyzed by real-time PCR using the Roche Sybr green quantification method. Results were normalized and presented as percentage of input DNA. The primers sequences used for amplification of potential HIF1 binding sites in *Sox9* and *Pgk1* (phosphoglycerate kinase 1) promoters are the following [relative to transcription start site (+1)]: *Sox9* amplicon A forward (-1949) GCCTTTGTGCCAGAATACGTGA, reverse (–1695) ACCCTGTAGCCTGTTTACGAGT; amplicon B forward (–917) TGTGACTCAGTCAGGAGGCAAGAA, reverse (–723) TGAAAACCAAAGCCGAGCACCA; amplicon C forward (–495) CATTGCTGTAAACGCCAGCGAA, reverse (–312) GTTTTGGAACGGTCTCCGTGTGAA; amplicon D forward (–102) TCAGCGACTTGCCAACACTGAT, reverse (+46) CCCACAGAAGTTTCCAGGCAGTT; *Pgk1* forward (–302) CCTCGCACACATTCCACATCCA, reverse TCAGCGACTTGCCAACACTGAT.

Formaldehyde cross-linked plasmid immunoprecipitation (plasmid IP)

pGL3-basic vector containing 2.8 kb of mouse *Sox9* proximal promoter was kindly provided by Dr C. Hartmann (Research Institute for Molecular Pathology, Vienna, Austria). Mutant constructs encoding a 4-nt substitution (CGTG to AAAA) were prepared in the context of the full-length *Sox9* promoter by PCR using the following primers: forward 5′-ATAGGTACCACGGAGACAGCATCGAAAAGTGGGGGTGGGGGGTTGTGGAGGGTCCTAGTCTAGACACGCTCGAAAACACGCGCACACACACAC-3′, reverse 5′-TCTCTCGAGCGACTTCCAGCTCAGGGTCTCTA-3′.

PCR was performed under the following conditions: 2 minutes at 94°C; 0.3 minutes at 94°C; 0.5 minutes at 55°C; 0.5 minutes at 72°C for 33 cycles and 5 minutes at 72°C. The PCR product was then digested with ACC65I and *Xho*I and ligated into pGL3-basic promoter. A 2.3 kb ACC65I–ACC65I was digested from the WT mouse *Sox9* promoter and ligated into ACC65I to construct a 2.8 kb *Sox9* promoter with mutated HRE.

At 70% confluence, 293A cells in a 100-mm dish were transfected with 1 μg of either WT or mutated pGL3 *Sox9* promoter and 3 μg of PEF-HIF1α P564A/N803A. At 30 hours after transfection, cells were fixed in normal culture medium with formaldehyde at a final concentration of 1% for 10 minutes at 37°C. Plasmid IP was perform as described previously (Ainbinder et al., 2004).

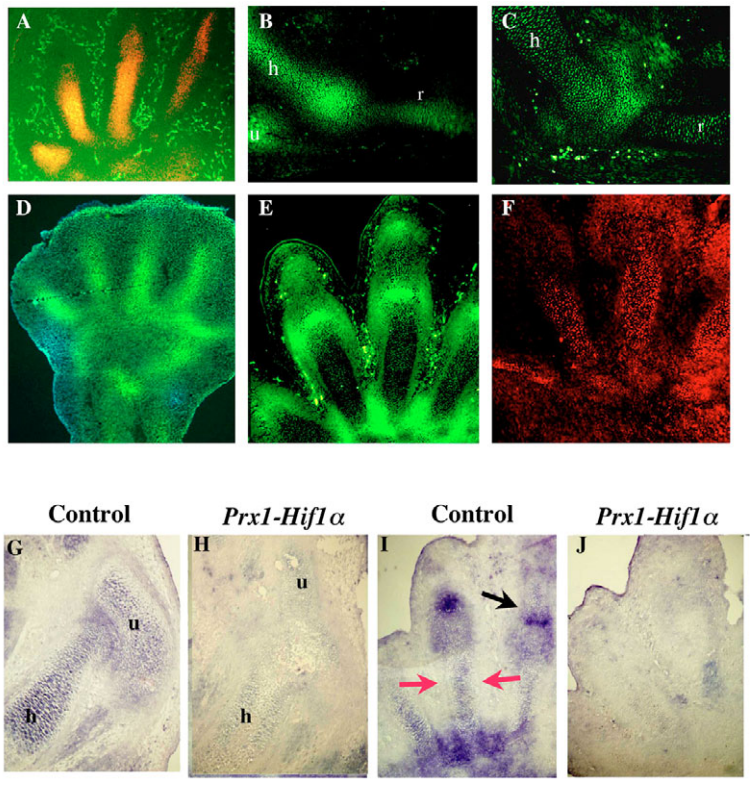

Fig. 1. HIF1α is expressed by hypoxic differentiating chondrocytes. (**A**) Sections of E12.5 autopod showing avascular cartilage. The vasculature was detected by immunofluorescence using anti-CD31 antibody (green); cartilage was detected by anti-collagen type II (red). (**B**,**C**) Sections through the elbow show hypoxic cells in the condensed mesenchyme at E11.5 (B) and E12.5 differentiating chondrocytes (C). (**D**,**E**) Section through the autopod at E12.5 (D) and E13.5 (E). Hypoxic cells were detected by immunofluorescence using Hypoxyprobe-1. (**F**) HIF1 detection in E13.5 digits by immunofluorescence using anti-HIF1α antibody. (**G-J**) *Pgk1* expression was detected by in situ hybridization on sections, showing the humerus region (G) and the digits (I) of E12.5 control. The expression was lost in humerus, ulna (H) and digits (J) of *Prx1-Cre-Hif1α* autopods. Black arrows indicate *Pgk1* expression in the interzone; red arrows indicate *Pgk1* expression in the inner part of the digit. h, humerus; r, radius; u, ulna.

RESULTS

Condensed mesenchymal cells in the limb are hypoxic and express *Hif1α*

Mesenchymal cells differentiate into chondrocytes in an avascular environment (Fig. 1A) (Feinberg et al., 1986; Hallmann et al., 1987). In order to examine whether the absence of vasculature at the condensation sites forces the condensed mesenchymal cells to differentiate under hypoxic conditions we used hypoxyprobe, a molecular marker that detects hypoxic cells (Arteel et al., 1998). Analysis of E11.5-E12.5 forelimbs identified a signal in the differentiating chondrocytes in the humerus, radius and ulna and in the condensing mesenchyme of the autopod (Fig. 1B-D). By E13.5 the signal was reduced, more prominently in the autopod, and it was elevated in the interzone of the forming joints (Fig. 1E). These results suggest that mesenchyme differentiation into chondrocytes and joint formation occur under low oxygen conditions.

The observation that differentiating mesenchymal cells, chondrocytes and cells of the forming joints are hypoxic led us to examine the expression of *Hif1α* and *Pgk1*, a bona fide *Hif1α* target gene, in these cells. Immunofluorescence analysis detected *Hif1α* expression in differentiating chondrocytes in the E13.5 autopod (Fig. 1F). *Pgk1* expression followed the pattern we observed using the hypoxyprobe, as it was detected in proximal elements of the limb and in the forming joints (Fig. 1G,I). Interestingly, *Pgk1* expression was observed in cells located at the center of the digits, whereas in the periphery the expression was reduced dramatically. *Pgk1* expression was lost in the autopod and the zeugopod upon inactivation of *Hif1α* in the limbs, indicating that the expression of *Pgk1* in the skeletal elements is HIF1α dependent (Fig. 1H,J). These results demonstrate that differentiating prechondrogenic cells in the limb are hypoxic and express *Hif1α*.

Lack of HIF1α in limb mesenchyme leads to impaired embryonic skeletal development

Finding that mesenchymal cell differentiation into chondrocytes and joint formation did take place under oxygen deprivation led us to study whether HIF1α is involved in the mechanism that supports differentiation under these conditions.

Using the *Prx1* promoter to drive the expression of *Cre* recombinase (Logan et al., 2002), we analyzed mice with a conditional deletion of *Hif1α* in limb bud mesenchyme. Embryos homozygous for *floxed-Hif1α* and heterozygous for *Prx1-Cre* alleles (*Prx1-Hif1α*) were compared with embryos heterozygous for *floxed-Hif1α* and *Prx1-Cre* alleles (control). Skeletal preparations of E18.5 *Prx1-Hif1α* embryos demonstrated a significant retardation in skeleton development relative to control: long bones were shorter, severely deformed and less mineralized, with joint fusion in elbow, knee and phalangeal joints (Fig. 2A-C). Examination of the autopod revealed severe defects in carpal and tarsal and digit formation. Cartilage formation was mostly identified in the periphery of the forming digits (Fig. 2C).

Histological examination of the *Prx1-Hif1α* limb confirmed the previously described role of HIF1α in chondrocyte survival (Schipani et al., 2001). Cell death in the proximal part of the skeleton was initiated at the joint region by E12.5 and was clearly visible at E13.5 (Fig. 2D and see Fig. S1 in the supplementary material). By E18.5 cell death at the joint region was extensive in most of the cartilaginous elements of the limb with the exception of the autopod (data not shown). In the autopod we observed only minor cell death, starting at E15.5 (see Fig. S1 in the supplementary material). At that stage we observed cells at

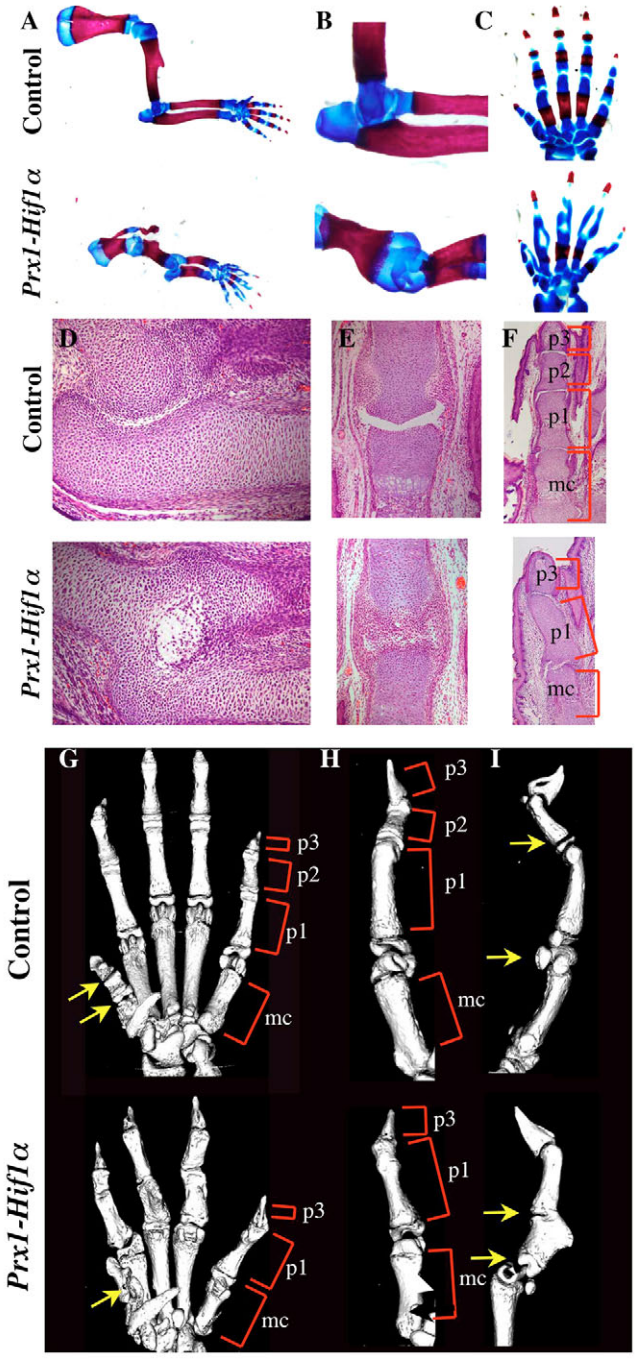

Fig. 2. Skeletal abnormalities in *Prx1-Hif1α* mutants. (**A-C**) Alizarin Red and Alcian Blue staining of wild-type (top) and *Prx1-Hif1α* (bottom) mouse forelimbs. E18.5 littermates demonstrate severe retardation in limb skeleton formation (A) and joint fusion (B). Autopod skeletons (C) show cartilage formation at the periphery of the forming digits and joint loss in the *Prx1-Cre-Hif1α* limb. (**D**) Histological sections of E13.5 control (top) and *Prx1-Cre-Hif1α* (bottom) elbows. In the *Prx1-Cre-Hif1α* joint, the presence of apoptotic cells with shrunken cytoplasm and condensed nuclei is observed. (**E**,**F**) Histological sections through the digits revealed partial joint cavitation (E) and loss of phalanx (F). (**G-I**) MicroCT analysis of 21-day-old *Prx1-Cre-Hif1α* and WT autopod: dorsal view demonstrates severe retardation in the *Prx1-Cre-Hif1α* skeleton including bone deformation, lack of phalanges (bracket), and joint fusion. H and I show dorsal and lateral views, respectively, of digit 3. Yellow arrows indicate fused joints and fused sesamoid bones.

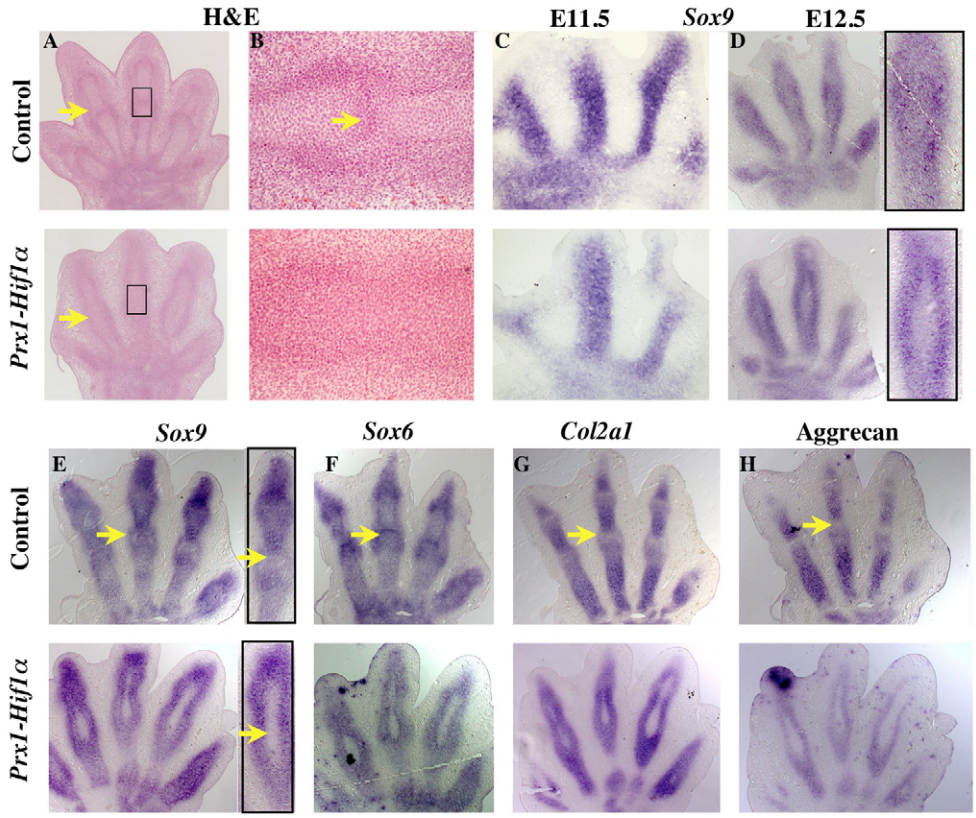

Fig. 3. HIF1α is necessary for chondrocyte differentiation. (**A**,**B**) Histology sections of E13.5 control (top) and *Prx1-Cre-Hif1α* (bottom) autopods showing mesenchyme-like morphology of the cells in *Prx1-Cre-Hif1α* digits. (B) Higher magnification of the boxed area in A demonstrates lack of interzone formation. (**C**,**D**) In situ hybridization for *Sox9*. (C) Uniform expression of *Sox9* in E11.5 mesenchymal condensation; (D) substantial reduction in *Sox9* expression in the center of E12.5 *Prx1-Cre-Hif1α* digits. (**E-H**) Serial sections of E13.5 control and *Prx1-Hif1α* autopods were hybridized with RNA probes for *Sox9* (E), *Sox6* (F), collagen type II (Col2a1; G) and aggrecan (H). Yellow arrows indicate the interzone.

the center of the digits that failed to differentiate, as they did not stain with Alcian Blue (see Fig. S2 in the supplementary material).

Blocking the expression of *Hif1α* in limb mesenchyme led to severe abnormalities in all skeletal elements (Fig. 2). However, the extensive chondrocyte cell death in the proximal skeletal elements prevented sufficient analysis of the direct roles of HIF1α in chondrogenesis. Our observation that cartilage formation in the autopod of the *Prx1-Hif1α* mouse occurred without noticeable cell death enabled us to study the possible roles of HIF1α in skeleton development regardless of its role in chondrocyte survival.

Further histological examination of the *Prx1-Hif1α* autopod revealed loss of phalanges in some of the digits (Fig. 2F). Some phalangeal joints were missing or only partially cavitated, whereas some of the joints that were cavitated lacked articular cartilage (Fig. 2E and see Fig. S1 in the supplementary material).

To evaluate the developmental abnormalities in the *Prx1-Hif1α* ossified skeleton we examined skeletons of post-natal day 21 mice by micro-CT. As can be seen in Fig. 2, the *Prx1-Hif1α* autopod digit five (D5) is missing one phalanx (Fig. 2G,H). In D3, the joint between the distal and the intermediate phalanges is partially fused (Fig. 2I). In addition, the metacarpophalangeal joints are severely deformed (Fig. 2G). In D1, the distal and the intermediate phalanges are fused and the joint is deformed (Fig. 2G). The sesamoid bones, which are located adjacent to the metacarpophalangeal joint, are fully or partially fused with the contiguous elements in the *Prx1-Hif1α* skeleton (Fig. 2G-I).

The severe abnormalities of *Prx1-Hif1α* skeleton strongly suggest that HIF1α plays a key role in the mechanism that regulates cartilage and joint formation.

HIF1α regulates the expression of *Sox9* in prechondrogenic cells

Histological examination of E13.5 *Prx1-Hif1α* sections of the autopod revealed cells that appeared as undifferentiated mesenchyme in the center of the forming digits. Furthermore, while the interzone, which marks the forming joint, had emerged in the control digits, it failed to appear in the *Prx1-Hif1α* digits (Fig. 3A,B).

To study the possibility that prechondrogenic cells in the *Prx1-Hif1α* forming digits cease to differentiate, we examined the expression of *Sox9* in E11.5-E13.5 *Prx1-Hif1α* autopods by section in situ hybridization. To date, *Sox9* is the earliest known marker for condensing mesenchyme. *Sox9* expression pattern in E11.5 *Prx1-Hif1α* limbs was comparable with the control limbs (Fig. 3C); by contrast, *Sox9* expression at E12.5 was noticeably altered: expression was observed only in the periphery outlining the forming phalanges, whereas at the center, where we observed undifferentiated mesenchymal cells, *Sox9* expression was dramatically reduced (Fig. 3D). By E13.5 the effect we had observed at E12.5 became much more noticeable (Fig. 3E). Concomitantly with the loss of *Sox9* expression, the expression of additional markers for chondrocyte differentiation, *Sox6*, collagen II and aggrecan, were lost as well (Fig. 3F-H). Interestingly, unlike in the control, when *Sox9* and collagen II expression was reduced at the sites where joints were forming, the *Prx1-Hif1α* sections lacked the *Sox9* and collagen II segmentation profile. *Sox6* expression at E13.5 seemed to increase in the forming joints of the control, but was missing in the *Prx1-Hif1α* sections, where digits also lacked the interzone (Fig. 3F).

The loss of *Sox9*, followed by the loss of *Sox6,* collagen II and aggrecan expression in the *Prx1-Hif1α* autopod strongly suggest that under hypoxic conditions HIF1α is necessary to maintain the differentiation program of prechondrogenic cells to chondrocytes.

Loss of *Hif1α* in limb mesenchyme affects chondrocyte proliferation

Previous experiments where *Sox9* expression was abolished in chondrocytes resulted in reduced chondrocyte proliferation (Akiyama et al., 2002). The reduction in both *Sox9* expression and the size of *Prx1-Hif1α* skeletal elements prompted us to examine whether the loss of HIF1α affected cell proliferation by assessing the incorporation of BrdU into the cells of the forming digits at E14.5. Whereas cell proliferation in the regions outside the forming digits was comparable in *Prx1-Hif1α* and control autopods, we observed a 3.5-fold reduction in the percentage of cell proliferation in *Prx1-Hif1α* digits, including the regions where joints were forming (Fig. 4B).

These results show that the abnormal differentiation of *Prx1-Hif1α* prechondrogenic cells to chondrocytes is associated with reduced cell proliferation.

Loss of *Hif1α* in limb mesenchyme results in abnormal interzone formation

Our observations of abnormal joint formation in the *Prx1-Hif1α* limb (Figs 2-4) led us to explore the involvement of HIF1α during early events of joint formation by examining the expression of *Gdf5*, a marker for joint formation (Storm and Kingsley, 1999). In E12.5 control autopods, *Gdf5* expression was mainly observed at joint formation sites and in the interdigital zone surrounding the forming condensation (Fig. 5A). By E13.5-E15.5, *Gdf5* expression was reduced outside the forming digits, and it was mostly observed in the developing joints (Fig. 5B-D,G). *Gdf5* expression in E12.5 *Prx1-Hif1α* limb was missing from the domains in which joints should have been developed, and was observed instead on the distal side of the developing digits; in the interdigital zone *Gdf5* expression was higher than in the control (Fig. 5A). By E13.5, the differences became more obvious: *Gdf5* expression in the interdigital zone was still prominent. In the *Prx1-Hif1α* digits, *Gdf5* expression could be observed on the distal side of the metacarpals, but instead of outlining the forming joint the expressing cells were located in the center of the digits (Fig. 5B,C). By E14.5-15.5, in some of the digits we detected indications of aberrant interzone formation; *Gdf5* expression domains were broader relative to the control, with indistinct borders (Fig. 5D,G). However, unlike in the control, we could not detect at that stage the expression of interzone markers such as *Wnt9a* or *Bmp2* in the *Prx1-Hif1α* joints (Fig. 5F-I).

Interestingly, the expression pattern of noggin, a GDF5 antagonist that is known to regulate cartilage and joint formation (Brunet et al., 1998), was also altered in *Prx1-Hif1α* limb. In E14.5 control autopod, noggin expression could be observed in prehypertrophic chondrocytes, epiphyseal chondrocytes and in the forming joints (Fig. 5E). In the *Prx1-Hif1α* limb, noggin expression was lost in the center of the forming digits but was instead present in the cells that outlined the digits (Fig. 5E). These results raise the possibility that joint abnormalities in *Prx1-Hif1α* limb are a consequence of interference with the GDF5-noggin signaling.

Vegf expression in limb mesenchyme is partially regulated by *Hif1α*

Vegf (vascular endothelial growth factor, also known as *Vegfa* – Mouse Genome Informatics) is a well-documented transcriptional target of HIF1α (Forsythe et al., 1996; Liu et al., 1995). To examine the possibility that HIF1α regulates *Vegf* expression in the limb and, as a consequence, regulates limb vasculature, we analyzed *Vegf* expression in E12.5 *Prx1-Hif1α* and control limbs by quantitative RT-PCR analysis. *Vegf* expression in the in *Prx1-Hif1α* limb was reduced by 30% relative to the control (Fig. 6C). To evaluate whether the reduction of *Vegf* in the *Prx1-Hif1α* limb caused vasculature abnormalities we examined vasculature development and patterning in the *Prx1-Hif1α* limb using sections double-stained with antibodies for PECAM (CD31) and collagen II to identify endothelial cells and chondrocytes, respectively. The vasculature in the *Prx1-Hif1α* autopod was comparable with that of the control (Fig. 6A,B); however, we observed a substantial decrease in collagen II expression that was well correlated with the reduction we detected in the collagen II mRNA level (Fig. 6B).

These results suggest that the regulation of *Vegf* and the vasculature in the limb is only partially regulated by HIF1α.

HIF1α is necessary for differentiation of mesenchymal precursors cells cultured under hypoxic conditions

The reduction in the expression of *Sox9*, *Sox6* and collagen II in the *Prx1-Hif1α* autopod strongly implies that HIF1α is required to maintain the differentiation of prechondrogenic cells to chondrocytes.

To unambiguously demonstrate that HIF1α is cell-autonomously required in mesenchymal precursors for their differentiation into chondrocytes we used high-density micromass culture as an in vitro model (DeLise et al., 2000). Micromass cultures derived from limb buds of *floxed-Hif1α* embryos were infected by either adeno-Cre virus (AdCre) to delete HIF1α, or adenovirus expressing GFP (AdGfp) as a control. To assess the efficiency of HIF1α deletion by AdCre we measured the expression of *Hif1α* and *Pgk1*, a defined

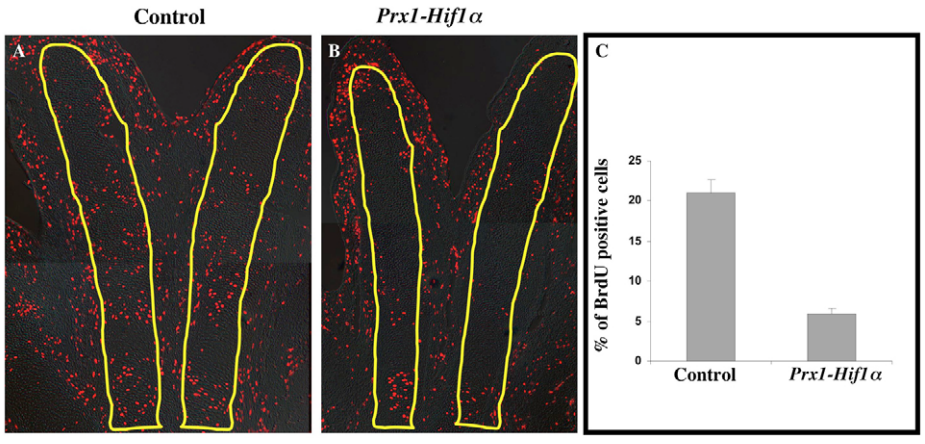

Fig. 4. Reduced chondrocyte proliferation in *Prx1-Hif1α* digits. BrdU incorporation into forming digits of control (**A**) and *Prx1-Hif1α* (**B**) mice. (**C**) Quantification of BrdU incorporation reveals a 3.5-fold reduction in the percentage of dividing cells in the mutant (control, 20.99±1.65%; *Prx-1-Hif1α*, 5.94±0.62%. $P<0.001$, $n=4$).

HIF1α target gene, using real-time PCR. Micromass cultures infected by AdCre or AdGfp were cultured under hypoxic or normoxic conditions. Under normoxic or hypoxic conditions the expression level of *Hif1α* in AdCre-infected cells was 25% and 12%, respectively, relative to the control (Fig. 7A). *Pgk1* expression level in control cells under hypoxic conditions increased more than twofold compared with normoxic levels, whereas in *Hif1α*-depleted cells this elevation was lost, as the level of expression was similar to normoxic values, suggesting an efficient blockage of HIF1α activity (Fig. 7B).

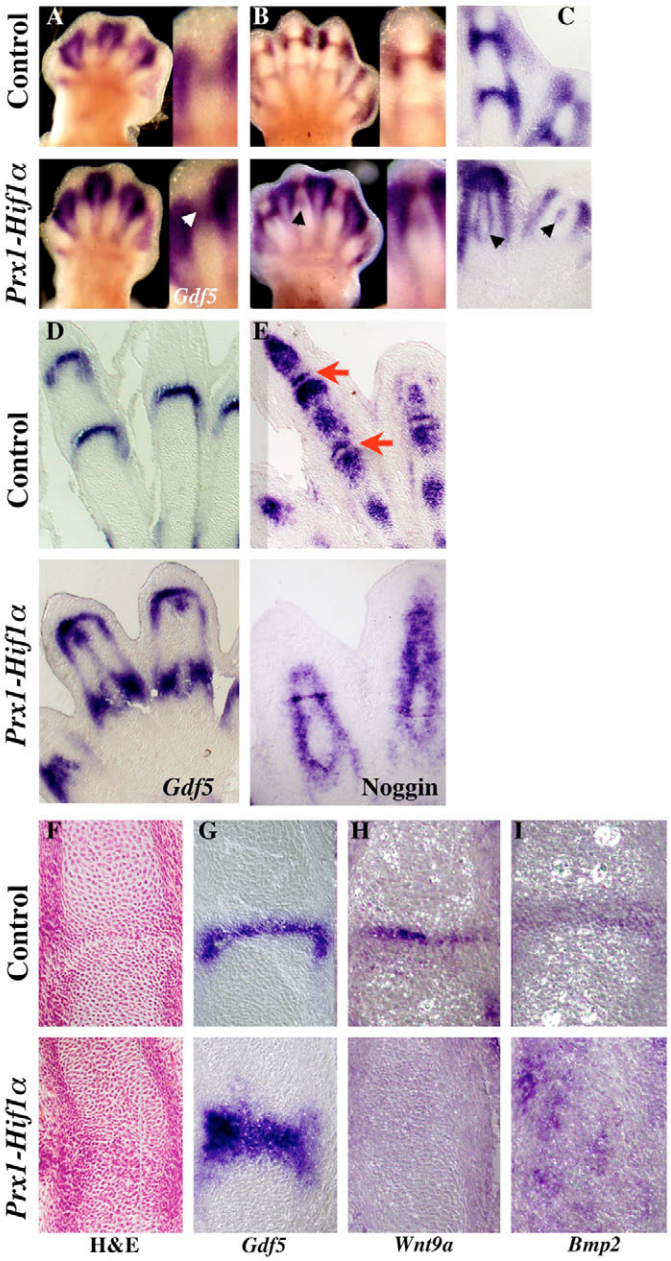

Fig. 5. Aberrant interzone formation in *Prx1-Hif1α* autopod. (**A-D**) In situ hybridizations for *Gdf5*. Whole-mount at E12.5 (A) and E13.5 (B) and sections at E13.5 (C) and E14.5 (D) show noticeable differences in the expression patterns between *Prx1-Hif1α* and control; white and black arrowheads indicate interzone area. (**E**) Noggin expression at E14.5. Red arrows indicate interzone area. (**F-I**) Higher magnification of the joint located between the first and the second phalanges of E15.5 control and *Prx1-Hif1α* autopods. (F) H&E staining. (G-I) Sections were hybridized with RNA probes for *Gdf5* (G), *Wnt9A* (H) and *Bmp2* (I).

Next, we studied the ability of *Hif1α*-depleted mesenchymal precursors to form cartilage nodules. Micromass cultures infected by AdCre or AdGfp were cultured under hypoxic or normoxic conditions and stained with Alcian Blue or tested by immunohistochemistry using collagen II antibody. As can be seen in Fig. 7C, in *Hif1α*-depleted cells under normoxia there was a mild reduction in nodule formation relative to control cells, whereas under hypoxic conditions, nodule formation by *Hif1α*-depleted cells was dramatically reduced. Next we examined the expression of collagen II and aggrecan, markers for chondrocyte differentiation, by quantitative RT-PCR. Interestingly, their expression showed a similar pattern to that of *Pgk1*. In control cells under hypoxic conditions their expression was elevated 1.6- and 2.3-fold, respectively, compared with normoxic levels, whereas in hypoxic *Hif1α*-depleted cells this increment was lost (Fig. 7D,E).

HIF1 directly regulates *Sox9* expression

The reduction in *Sox9* expression in vivo along with the expression pattern of *Sox9* target genes collagen II and aggrecan in vitro, led us to investigate whether HIF1 regulates *Sox9* expression. First we studied the ability of *Hif1α* overexpression to increase *Sox9* expression under normoxic conditions. *Sox9* expression in micromass cultures infected with either lentivirus (Lv)-HIF1α or Lv-Gfp (control) was examined by quantitative RT-PCR. In cells infected with Lv-HIF1α the expression of *Sox9* was elevated twofold, similar to *Pgk1*, a bona fide HIF1α target gene (Fig. 8A).

To further establish the regulation of *Sox9* by HIF1α, the expression of *Sox9* in *Hif1α*-depleted cells was examined by quantitative RT-PCR and western blot analysis. Under normoxia, in *Hif1α*-depleted cells there was a 29% reduction in the expression of *Sox9* relative to the control (Fig. 8B). Under hypoxic conditions there was a twofold increment in *Sox9* expression in control cells, whereas in *Hif1α*-depleted cells the elevation was lost as the level of expression was similar to normoxic values (Fig. 8B). Concomitantly with the lack of *Sox9* mRNA induction in *Hif1α*-depleted cells, under hypoxic conditions SOX9 protein level was dramatically reduced (Fig. 8C). Next we examined the expression of *Sox5* and *Sox6*; as can be seen in Fig. 8D,E, their expression profile followed *Sox9* expression. Under normoxia, in *Hif1α*-depleted cells there was a mild reduction in the expression of *Sox5* and *Sox6* relative to the control. Under hypoxic conditions there was a 2.3-fold increment in *Sox5* expression and 1.6-fold increment in *Sox6* expression in control cells, whereas in the *Hif1α*-depleted cells the level of expression was similar to values measured under normoxic conditions.

In order to examine whether HIF1α directly regulated *Sox9* expression we searched the mouse *Sox9* promoter for HIF1 consensus binding sites (also referred to as hypoxia response elements or HRE) (Wenger et al., 2005). We identified four putative binding sites within 3.0 kb upstream to the transcription initiation site (Fig. 8F). In order to examine whether HIF1α binds to one or more of the putative sequences, chromatin immunoprecipitation (ChIP) was performed using lysate from micromass cells cultured under either hypoxia or normoxia. The lysate was incubated with either an anti-HIF1α antibody or anti β-galactosidase antibody (as control). As a positive control we demonstrated binding of HIF1α to *Pgk1*, in chromatin from hypoxic cells (see Fig. S2 in the supplementary material). Our analysis revealed that HIF1α bound to an HRE sequence located 398 bp upstream of the transcription

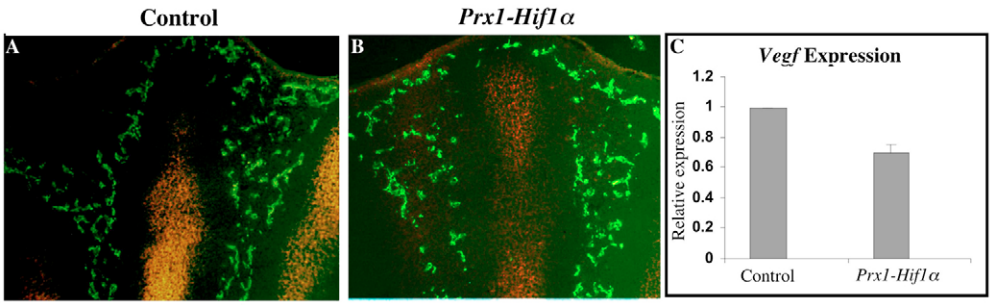

Fig. 6. *Vegf* expression and vasculature formation in *Hif1α*-deleted limb. Immunofluorescence of E12.5 sections of control (**A**) and *Prx1-Cre-Hif1α* (**B**) mouse limbs using antibodies for collagen type II (red) and CD31 (green). (**C**) Quantitative RT-PCR demonstrates reduction in *Vegf* mRNA level in *Prx1-Cre-Hif1α* E12.5 limbs (*n*=2).

initiation site (HRE 398). The other three HRE binding sites did not reveal any significant binding (Fig. 8G,H). Interestingly, HIF1α bound to HRE 398 sequence under normoxia as well, although with lower affinity. This result might explain the reduction in *Sox9* mRNA level that we observed in cells cultured under normoxia (Fig. 8B).

To further demonstrate the specificity of the HIF1α consensus binding site that we identified in the *Sox9* promoter, we substituted four nucleotides in the core consensus sequence of HRE 398 and examined HIF1α binding to the mutated *Sox9* promoter using a plasmid IP experiment. HIF1α binding was evaluated in 293A cells that were co-transfected with an HIF1α-expressing plasmid and with plasmids that contained either the WT *Sox9* promoter or a *Sox9* promoter with mutations in HRE 398. We detected HIF1α binding to the HRE 398 region in cells that were transfected with the control *Sox9* promoter; the binding was lost once the HRE 398 site was mutated (Fig. 8I).

These results indicate that HIF1α directly regulates *Sox9* expression. In addition, they show that HIF1α-dependent regulation of *Sox9* is necessary to maintain *Sox5* and *Sox6* expression under hypoxic conditions.

DISCUSSION

In this study we describe how an early step in skeletogenesis, namely mesenchymal cell differentiation, which occurs under oxygen deprivation, is regulated by HIF1α. *Hif1α* deletion in limb mesenchyme led to dramatic reduction in *Sox9* expression followed by differentiation arrest that resulted in severe skeletal malformations. Using micromass cultures as an in vitro model for chondrogenesis we found that HIF1α directly regulated *Sox9* expression, thus providing a molecular mechanism for the abnormalities observed in *Prx1-Hif1α* limbs. These findings establish HIF1α as a key component in the mechanism that regulates embryonic chondrogenesis.

Hypoxia and development

Until the establishment of a connection with maternal blood supply at E8.5, the murine embryo experiences low oxygen tension within the hypoxic range. At later stages of development, organ growth that precedes vascular development leads to hypoxic micro-environments (Maltepe and Simon, 1998; Mitchell and Yochim, 1968; Rodesch et al., 1992). During evolution, several organs have adapted to hypoxic developmental conditions and integrated hypoxia into their intrinsic genetic program as an external regulatory signal. Organs such as the neural tube (Hogan et al., 2004), placenta (Cowden Dahl et al., 2005; Ambati et al., 2006) and skeleton develop in the absence of embedded vasculature. The hypoxic niches that are formed directly affect the developmental process of each specific organ. The most profound effect of hypoxia during organogenesis is the regulation of differentiation and proliferation of progenitor cells. Hypoxia may either promote or inhibit differentiation in a cell-type-specific manner. For example, whereas hypoxia prevents the differentiation of hES cells (Ezashi et al., 2005) and inhibits myogenesis (Gustafsson et al., 2005), osteogenesis (D'Ippolito et al., 2006; Salim et al., 2004) and adipogenesis (Yun et al., 2002), it promotes the differentiation of mesencephalic precursors (Studer et al., 2000) and enhances hemangioblast specification (Ramirez-Bergeron et al., 2004).

In order to sense oxygen tension and convert the information into a cellular response, cells have developed a molecular signaling pathway in which HIF1 is an essential component (Semenza, 2004). Evidence for the significance of this pathway in embryonic development came from genetic studies. Null mutations in *Hif1* subunits led to early embryonic lethality due to placental failure, neural tube and vascular defects (Maltepe et al., 1997; Semenza et al., 1999). More recent studies have provided molecular insight into the role of HIF1 in the developmental response to hypoxia. Under hypoxia, HIF1 upregulates the expression of *Vegf*, *Flk-1* (also known as *Kdr* – Mouse Genome Informatics) and erythropoietin, as well as other genes involved in vascular development (Maltepe and Simon, 1998). This molecular response is essential for the proper differentiation and maintenance of the cardiovascular system. HIF1α inhibits the differentiation of myogenic and neural precursor cell lines by enhancing Notch signaling (Gustafsson et al., 2005) and prevents adipocyte differentiation by inhibiting PPARγ2 expression (Yun et al., 2002).

During initial stages of skeletogenesis the prechondrogenic condensations are avascularized and, as shown in our work, hypoxic. Our study provides direct evidence for the key role of HIF1α in the mechanism that has been developed by prechondrogenic cells to support their differentiation into chondrocytes and joint-forming cells. More specifically, under hypoxic conditions HIF1α is necessary to regulate the expression of the key chondrogenic regulator *Sox9,* in order to maintain chondrogenesis.

However, one interesting question that still remains to be resolved is the evolutionary explanation for the selection of a genetic program that dictates and requires that the chondrogenic process should take place under hypoxic conditions. Although we have no definite answer, we favor the possibility that the driving force behind this selection is to enhance the robustness of the genetic program that regulates chondrogenesis. Limb mesenchyme can differentiate to various lineages including chondrocytes, osteoblasts and tendon-forming cells. It is possible that whereas hypoxia inhibits differentiation of limb mesenchymal cells as a whole (D'Ippolito et al., 2006; Salim et al., 2004), the chondrogenic lineage escapes this inhibition because of the regulation of *Sox9* by *Hif1α*.

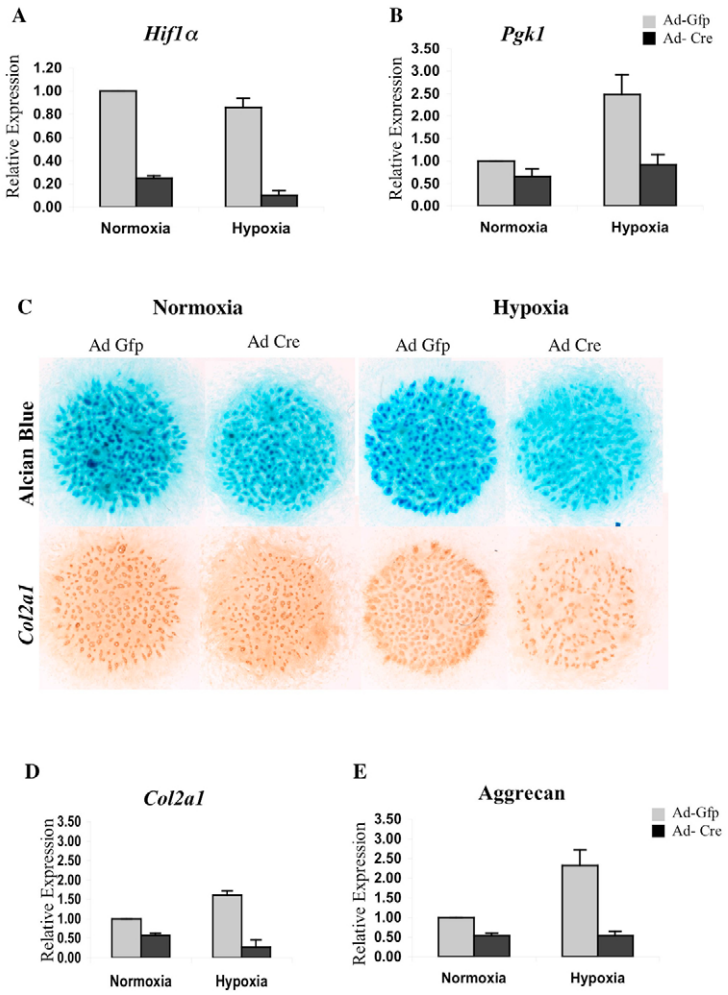

Fig. 7. HIF1α is necessary for mesenchymal cell differentiation under hypoxia. (**A**,**B**) Micromass culture of mesenchymal cells derived from E11.5 *Hif1α* floxed/floxed mouse embryos were infected with AdCre or AdGfp (control) and were cultured under normoxic (20% O_2) or hypoxic (1% O_2) conditions as indicated (gray, AdGfp; black, AdCre). Quantitative RT-PCR shows deletion of *Hif1α* (A) and loss of *Pgk1* induction under hypoxia (B) in AdCre-infected cells relative to AdGfp-infected cells. (**C**) Alcian Blue staining (above) and immunohistochemical staining for collagen type II (Col2a1; below) reveal reduction in cartilage nodule formation in AdCre-infected cells cultured under hypoxia. (**D**,**E**) Substantial reduction in collagen II (D) and aggrecan (E) mRNA is detected by quantitative RT-PCR (*n*=3).

The involvement of HIF1α in joint formation

The emergence of the interzone is the first histological indication of joint formation (Mitrovic, 1977). Molecularly, the expression of the chondrogenic markers *Sox9*, collagen II and aggrecan decreases in interzone cells, whereas the expression of *Gdf5*, noggin, *Wnt9A* and *Bmp2* is elevated. In our study, both histological and molecular examinations of Prx*1-Hif1α* autopods showed abnormal interzone formation (Fig. 5).

Abnormal joint formation in the *Prx1-Hif1α* limb may result from the reduction in *Sox9* and the consequent failure of prechondrogenic cells to differentiate to chondrocytes. This suggests that the ability of condensed mesenchymal cells to adopt interzone cell fate depends on proper differentiation of the flanking cells into chondrocytes. Studies where SOX9 was inactivated in prechondrocytes support this possibility: severe reduction in cartilage formation was followed by fusion of the carpal elements and low expression levels of noggin, *Gdf5* and *Wnt9a* (Akiyama et al., 2002).

An alternative explanation may lie in our observation of abnormal expression of *Gdf5* and noggin (Fig. 5A-E). It has been shown that alterations in either the expression or activity of these two genes resulted in multiple joint defects (Kjaer et al., 2006; Lehmann et al., 2003; Seemann et al., 2005). *Gdf5* misexpression by implantation of beads into the interdigital region of E12.5 embryos resulted in interference in metacarpophalangeal joint development, with reduction in the expression of joint markers and increase in the expression of chondrogenic markers (Storm and Kingsley, 1999). Noggin haploinsufficiency was recently reported to lead to carpal and tarsal joint fusions (Tylzanowski et al., 2006). Human genetic studies further support this hypothesis: point mutations that altered the activity of GDF5 and its antagonist noggin resulted in brachydactyly and symphalangism (Gong et al., 1999; Marcelino et al., 2001; Seemann et al., 2005). The expression of *Gdf5* in *Prx1-Hif1α* limbs in our study rules out the possibility that HIF1α is necessary for its expression (Fig. 5A-D). Nevertheless, the alterations we observed in *Gdf5* and noggin expression patterns in *Prx1-Hif1α* limbs may indicate that in the absence of HIF1α the fine balance between noggin and GDF5 is disturbed, causing aberrations in joint formation.

HIF1α regulates chondrocyte differentiation

Mesenchymal condensation is the initial step in cartilage formation, and SOX9 is an essential regulator of this process (Akiyama et al., 2002). Our finding that *Prx1-Hif1α* limb mesenchymal cells did condense and initially expressed *Sox9* (Fig. 3C) suggests that HIF1α is not necessary for chondrocyte cell fate determination. However, later in development *Sox9* expression is further required to regulate the differentiation of prechondrogenic cells into chondrocytes. Our histological observation of cells that appeared as undifferentiated mesenchyme and lacked *Sox9* expression in the *Prx1-Hif1α* autopod implies that HIF1α is necessary to sustain the chondrogenic program by maintaining *Sox9* expression in these cells (Fig. 3D,E)

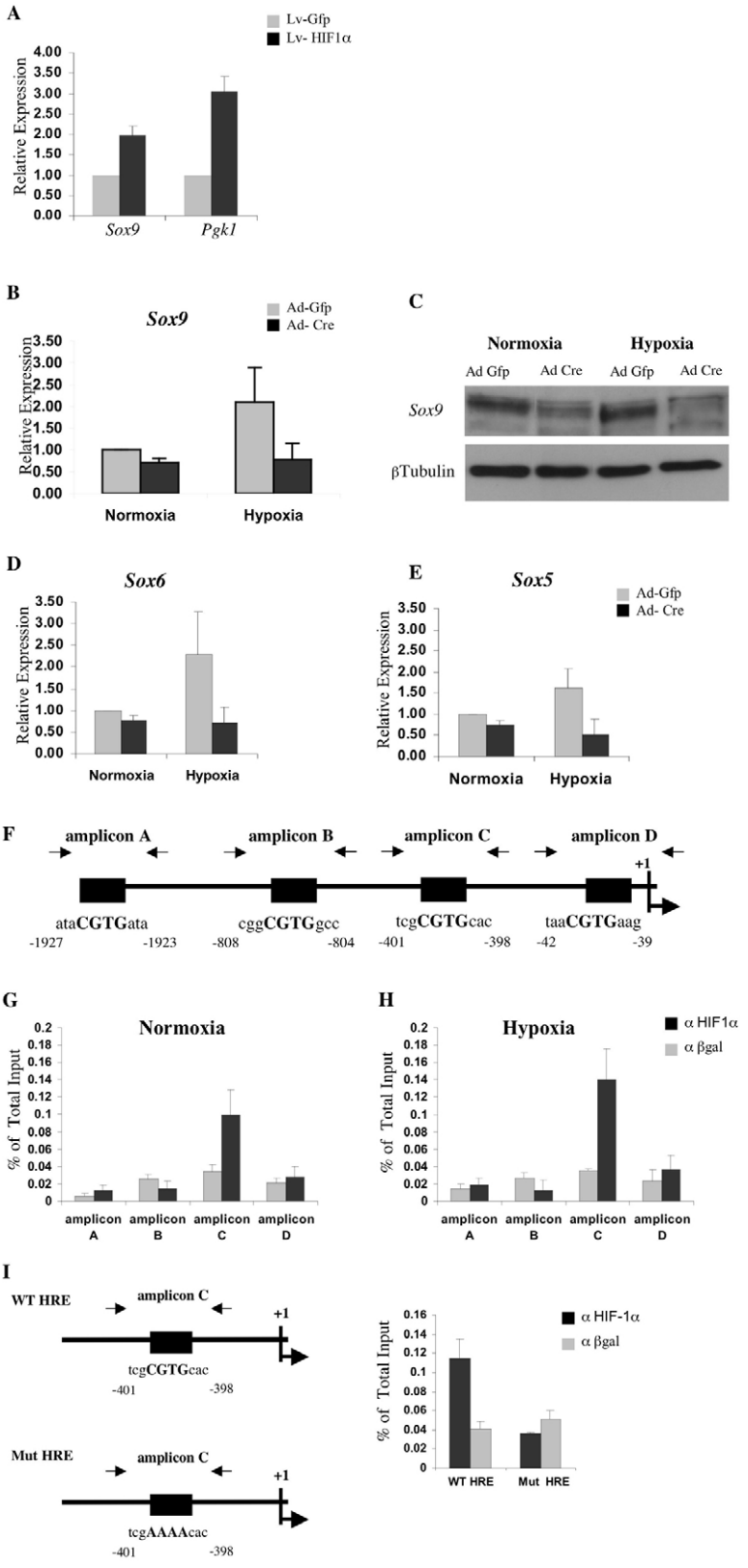

Fig. 8. HIF1α directly regulates *Sox9* expression. (**A**) Increase in *Sox9* and *Pgk1* mRNA level upon infection of mesenchymal cells with lentivirus encoding stabilized human HIF1α (*n*=2). (**B**,**C**) Substantial reduction in *Sox9* mRNA and protein level in AdCre-infected cells was detected by quantitative RT-PCR analysis (B) and immunoblot assay (C). (**D**,**E**) Quantitative RT-PCR analyses for *Sox6* (D) and *Sox5* (E) show a marked decrease in AdCre-infected cells under hypoxia (*n*=3). (**F**) Schematic view of 3.0 kb *Sox9* promoter region showing the position of four potential HIF1α binding sites relative to the transcription start site. (**G**,**H**) Chromatin immunoprecipitation assay of mouse *Sox9* gene. Real-time PCR quantification of *Hif1α* binding to regions A-D (amplicons) is indicated by the percentage of total input chromatin DNA (*n*=2). (**I**) Immunoprecipitation assay with plasmids that contain control *Sox9* promoter or plasmids that contain the *Sox9* promoter with a four-nucleotide substitution in the HRE 398 (*n*=2).

Micromass culture experiments further supported the role of HIF1α in regulating the transition of prechondrogenic cells to chondrocytes by regulating *Sox9* expression. Under hypoxia, cartilage nodule formation by *Hif1α*-deleted mesenchymal cells was dramatically reduced relative to the control (Fig. 7C). Quantitative real-time PCR revealed an HIF1α-dependent induction of *Sox9* expression under hypoxic conditions (Fig. 8B). Moreover, forced expression of HIF1α in these cells resulted in a twofold increase in *Sox9* mRNA level. These results suggest that HIF1α is necessary to maintain the *Sox9* mRNA level under hypoxic conditions (Fig. 8B,C).

Following the same pattern, the expression of *Sox5*, *Sox6* (Fig. 8C,D), collagen II and aggrecan (Fig. 7D,E) were elevated in control mesenchymal cells under hypoxic conditions in a HIF1α-dependent manner, as this elevation failed to occur in *Hif1α*-deleted cells.

A previous study demonstrated that hypoxia could increase the activity of the *Sox9* proximal promoter in ST2 cell line. The increment was lost when the HIF1 consensus binding site in the promoter was mutated (Robins et al., 2005). Our analysis revealed four putative HIF1 consensus binding sites in a genomic region spanning 3.0 kb upstream to transcription start site. ChIP and plasmid IP analyses provided evidence for direct interaction of HIF1α with one out of the four sites identified (Fig. 8H,I). Interestingly, Robins et al. identified the same element as a potential HIF1 binding site, thus providing additional and independent support for the direct regulation of *Sox9* expression by HIF1α.

With the exception of the three members of the SOX transcription factors family, namely: SOX9, SOX5 and SOX6, very little is known about the transcriptional machinery that regulates the various differentiation steps leading to the formation of a functional chondrocyte. Finding both in vitro and in vivo that the differentiation of mesenchymal cells to chondrocytes required *Hif1α* expression suggests that HIF1α is an essential component in the transcriptional mechanism that regulates the transition of prechondrogenic cells to chondrocytes.

We are grateful to Dr C. Tabin for the *Prx1-Cre* mice, to Dr C. Hartmann for the mouse *Sox9* proximal promoter and RNA probes, to Dr V. Lefebvre for RNA probes, to Dr Inder M. Verma for lentiviral transfer vector, to Dr A. Chen for helpful suggestions in constructing and producing lentiviruses, to Dr H. Akiyama for Ad-Sox9 virus constructs and to Dr M. Whitelaw for HIF1α expression plasmids. We thank Ms S. Kerief for expert technical support, Mr N. Konstantin for expert editorial assistance and members of the Zelzer laboratory for advice and suggestions. This work was supported by Israel Science Foundation grant 499/05, Minerva grant M941, The Leo and Julia Forchheimer Center for Molecular Genetics, The Stanley Chais New Scientist Fund and The Women's Health Research Center. E.Z. is the incumbent of the Martha S. Sagon Career Development Chair.

Supplementary material

Supplementary material for this article is available at http://dev.biologists.org/cgi/content/full/134/21/3917/DC1

References

Ainbinder, E., Amir-Zilberstein, L., Yamaguchi, Y., Handa, H. and Dikstein, R. (2004). Elongation inhibition by DRB sensitivity-inducing factor is regulated by the A20 promoter via a novel negative element and NF-kappaB. *Mol. Cell. Biol.* **24**, 2444-2454.

Akiyama, H., Chaboissier, M. C., Martin, J. F., Schedl, A. and de Crombrugghe, B. (2002). The transcription factor Sox9 has essential roles in successive steps of the chondrocyte differentiation pathway and is required for expression of Sox5 and Sox6. *Genes Dev.* **16**, 2813-2828.

Ambati, B. K., Nozaki, M., Singh, N., Takeda, A., Jani, P. D., Suthar, T., Albuquerque, R. J., Richter, E., Sakurai, E., Newcomb, M. T. et al. (2006). Corneal avascularity is due to soluble VEGF receptor-1. *Nature* **443**, 993-997.

Archer, C. W., Dowthwaite, G. P. and Francis-West, P. (2003). Development of synovial joints. *Birth Defects Res. C Embryo Today* **69**, 144-155.

Arteel, G. E., Thurman, R. G. and Raleigh, J. A. (1998). Reductive metabolism of the hypoxia marker pimonidazole is regulated by oxygen tension independent of the pyridine nucleotide redox state. *Eur. J. Biochem.* **253**, 743-750.

Bi, W., Deng, J. M., Zhang, Z., Behringer, R. R. and de Crombrugghe, B. (1999). Sox9 is required for cartilage formation. *Nat. Genet.* **22**, 85-89.

Brunet, L. J., McMahon, J. A., McMahon, A. P. and Harland, R. M. (1998). Noggin, cartilage morphogenesis, and joint formation in the mammalian skeleton. *Science* **280**, 1455-1457.

Cowden Dahl, K. D., Fryer, B. H., Mack, F. A., Compernolle, V., Maltepe, E., Adelman, D. M., Carmeliet, P. and Simon, M. C. (2005). Hypoxia-inducible factors 1alpha and 2alpha regulate trophoblast differentiation. *Mol. Cell. Biol.* **25**, 10479-10491.

D'Ippolito, G., Diabira, S., Howard, G. A., Roos, B. A. and Schiller, P. C. (2006). Low oxygen tension inhibits osteogenic differentiation and enhances stemness of human MIAMI cells. *Bone* **39**, 513-522.

DeLise, A. M., Stringa, E., Woodward, W. A., Mello, M. A. and Tuan, R. S. (2000). Embryonic limb mesenchyme micromass culture as an in vitro model for chondrogenesis and cartilage maturation. *Methods Mol. Biol.* **137**, 359-375.

Ezashi, T., Das, P. and Roberts, R. M. (2005). Low O_2 tensions and the prevention of differentiation of hES cells. *Proc. Natl. Acad. Sci. USA* **102**, 4783-4788.

Feinberg, R. N., Latker, C. H. and Beebe, D. C. (1986). Localized vascular regression during limb morphogenesis in the chicken embryo. I. Spatial and temporal changes in the vascular pattern. *Anat. Rec.* **214**, 405-409.

Forsythe, J. A., Jiang, B. H., Iyer, N. V., Agani, F., Leung, S. W., Koos, R. D. and Semenza, G. L. (1996). Activation of vascular endothelial growth factor gene transcription by hypoxia-inducible factor 1. *Mol. Cell. Biol.* **16**, 4604-4613.

Gong, Y., Krakow, D., Marcelino, J., Wilkin, D., Chitayat, D., Babul-Hirji, R., Hudgins, L., Cremers, C. W., Cremers, F. P., Brunner, H. G. et al. (1999). Heterozygous mutations in the gene encoding noggin affect human joint morphogenesis. *Nat. Genet.* **21**, 302-304.

Gustafsson, M. V., Zheng, X., Pereira, T., Gradin, K., Jin, S., Lundkvist, J., Ruas, J. L., Poellinger, L., Lendahl, U. and Bondesson, M. (2005). Hypoxia requires notch signaling to maintain the undifferentiated cell state. *Dev. Cell* **9**, 617-628.

Hallmann, R., Feinberg, R. N., Latker, C. H., Sasse, J. and Risau, W. (1987). Regression of blood vessels precedes cartilage differentiation during chick limb development. *Differentiation* **34**, 98-105.

Hartmann, C. and Tabin, C. J. (2001). Wnt-14 plays a pivotal role in inducing synovial joint formation in the developing appendicular skeleton. *Cell* **104**, 341-351.

Hogan, K. A., Ambler, C. A., Chapman, D. L. and Bautch, V. L. (2004). The neural tube patterns vessels developmentally using the VEGF signaling pathway. *Development* **131**, 1503-1513.

Jaakkola, P., Mole, D. R., Tian, Y. M., Wilson, M. I., Gielbert, J., Gaskell, S. J., Kriegsheim, A., Hebestreit, H. F., Mukherji, M., Schofield, C. J. et al. (2001). Targeting of HIF-alpha to the von Hippel-Lindau ubiquitylation complex by O_2-regulated prolyl hydroxylation. *Science* **292**, 468-472.

Karsenty, G. and Wagner, E. F. (2002). Reaching a genetic and molecular understanding of skeletal development. *Dev. Cell* **2**, 389-406.

Kjaer, K. W., Eiberg, H., Hansen, L., van der Hagen, C. B., Rosendahl, K., Tommerup, N. and Mundlos, S. (2006). A mutation in the receptor binding site of GDF5 causes Mohr-Wriedt brachydactyly type A2. *J. Med. Genet.* **43**, 225-231.

Kronenberg, H. M. (2003). Developmental regulation of the growth plate. *Nature* **423**, 332-336.

Lehmann, K., Seemann, P., Stricker, S., Sammar, M., Meyer, B., Suring, K., Majewski, F., Tinschert, S., Grzeschik, K. H., Muller, D. et al. (2003). Mutations in bone morphogenetic protein receptor 1B cause brachydactyly type A2. *Proc. Natl. Acad. Sci. USA* **100**, 12277-12282.

Liu, Y., Cox, S. R., Morita, T. and Kourembanas, S. (1995). Hypoxia regulates vascular endothelial growth factor gene expression in endothelial cells. Identification of a 5′ enhancer. *Circ. Res.* **77**, 638-643.

Logan, M., Martin, J. F., Nagy, A., Lobe, C., Olson, E. N. and Tabin, C. J. (2002). Expression of Cre recombinase in the developing mouse limb bud driven by a Prxl enhancer. *Genesis* **33**, 77-80.

Maltepe, E. and Simon, M. C. (1998). Oxygen, genes, and development: an analysis of the role of hypoxic gene regulation during murine vascular development. *J. Mol. Med.* **76**, 391-401.

Maltepe, E., Schmidt, J. V., Baunoch, D., Bradfield, C. A. and Simon, M. C. (1997). Abnormal angiogenesis and responses to glucose and oxygen deprivation in mice lacking the protein ARNT. *Nature* **386**, 403-407.

Marcelino, J., Sciortino, C. M., Romero, M. F., Ulatowski, L. M., Ballock, R. T., Economides, A. N., Eimon, P. M., Harland, R. M. and Warman, M. L. (2001). Human disease-causing NOG missense mutations: effects on noggin secretion, dimer formation, and bone morphogenetic protein binding. *Proc. Natl. Acad. Sci. USA* **98**, 11353-11358.

McLeod, M. J. (1980). Differential staining of cartilage and bone in whole mouse fetuses by alcian blue and alizarin red S. *Teratology* **22**, 299-301.

Mitchell, J. A. and Yochim, J. M. (1968). Measurement of intrauterine oxygen tension in the rat and its regulation by ovarian steroid hormones. *Endocrinology* **83**, 691-700.

Mitrovic, D. R. (1977). Development of the metatarsophalangeal joint of the chick embryo: morphological, ultrastructural and histochemical studies. *Am. J. Anat.* **150**, 333-347.

Mori-Akiyama, Y., Akiyama, H., Rowitch, D. H. and de Crombrugghe, B. (2003). Sox9 is required for determination of the chondrogenic cell lineage in the cranial neural crest. *Proc. Natl. Acad. Sci. USA* **100**, 9360-9365.

Murtaugh, L. C., Chyung, J. H. and Lassar, A. B. (1999). Sonic hedgehog promotes somitic chondrogenesis by altering the cellular response to BMP signaling. *Genes Dev.* **13**, 225-237.

Olsen, B. R., Reginato, A. M. and Wang, W. (2000). Bone development. *Annu. Rev. Cell Dev. Biol.* **16**, 191-220.

Oster, G. F., Shubin, N., Murray, J. D. and Alberch, P. (1988). Evolution and

morphogenetic rules: the shape of the vertebrate limb in ontogeny and phylogeny. *Evolution* **42**, 862-884.
Pacifici, M., Koyama, E. and Iwamoto, M. (2005). Mechanisms of synovial joint and articular cartilage formation: recent advances, but many lingering mysteries. *Birth Defects Res. C Embryo Today* **75**, 237-248.
Ramirez-Bergeron, D. L., Runge, A., Dahl, K. D., Fehling, H. J., Keller, G. and Simon, M. C. (2004). Hypoxia affects mesoderm and enhances hemangioblast specification during early development. *Development* **131**, 4623-4634.
Riddle, R. D., Johnson, R. L., Laufer, E. and Tabin, C. (1993). Sonic hedgehog mediates the polarizing activity of the ZPA. *Cell* **75**, 1401-1416.
Robins, J. C., Akeno, N., Mukherjee, A., Dalal, R. R., Aronow, B. J., Koopman, P. and Clemens, T. L. (2005). Hypoxia induces chondrocyte-specific gene expression in mesenchymal cells in association with transcriptional activation of Sox9. *Bone* **37**, 313-322.
Rodesch, F., Simon, P., Donner, C. and Jauniaux, E. (1992). Oxygen measurements in endometrial and trophoblastic tissues during early pregnancy. *Obstet. Gynecol.* **80**, 283-285.
Ryan, H. E., Poloni, M., McNulty, W., Elson, D., Gassmann, M., Arbeit, J. M. and Johnson, R. S. (2000). Hypoxia-inducible factor-1alpha is a positive factor in solid tumor growth. *Cancer Res.* **60**, 4010-4015.
Salim, A., Nacamuli, R. P., Morgan, E. F., Giaccia, A. J. and Longaker, M. T. (2004). Transient changes in oxygen tension inhibit osteogenic differentiation and Runx2 expression in osteoblasts. *J. Biol. Chem.* **279**, 40007-40016.
Schipani, E., Ryan, H. E., Didrickson, S., Kobayashi, T., Knight, M. and Johnson, R. S. (2001). Hypoxia in cartilage: HIF-1alpha is essential for chondrocyte growth arrest and survival. *Genes Dev.* **15**, 2865-2876.
Schofield, C. J. and Ratcliffe, P. J. (2004). Oxygen sensing by HIF hydroxylases. *Nat. Rev. Mol. Cell Biol.* **5**, 343-354.
Seemann, P., Schwappacher, R., Kjaer, K. W., Krakow, D., Lehmann, K., Dawson, K., Stricker, S., Pohl, J., Ploger, F., Staub, E. et al. (2005). Activating and deactivating mutations in the receptor interaction site of GDF5 cause symphalangism or brachydactyly type A2. *J. Clin. Invest.* **115**, 2373-2381.
Semenza, G. L. (1998). Hypoxia-inducible factor 1, master regulator of O_2 homeostasis. *Curr. Opin. Genet. Dev.* **8**, 588-594.
Semenza, G. L. (2003). Targeting HIF-1 for cancer therapy. *Nat. Rev. Cancer* **3**, 721-732.
Semenza, G. L. (2004). Hydroxylation of HIF-1: oxygen sensing at the molecular level. *Physiology Bethesda* **19**, 176-182.
Semenza, G. L., Agani, F., Iyer, N., Kotch, L., Laughner, E., Leung, S. and Yu, A. (1999). Regulation of cardiovascular development and physiology by hypoxia-inducible factor 1. *Ann. N. Y. Acad. Sci.* **874**, 262-268.
Smits, P., Li, P., Mandel, J., Zhang, Z., Deng, J. M., Behringer, R. R., de Crombrugghe, B. and Lefebvre, V. (2001). The transcription factors L-Sox5 and Sox6 are essential for cartilage formation. *Dev. Cell* **1**, 277-290.
Storm, E. E. and Kingsley, D. M. (1999). GDF5 coordinates bone and joint formation during digit development. *Dev. Biol.* **209**, 11-27.
Studer, L., Csete, M., Lee, S. H., Kabbani, N., Walikonis, J., Wold, B. and McKay, R. (2000). Enhanced proliferation, survival, and dopaminergic differentiation of CNS precursors in lowered oxygen. *J. Neurosci.* **20**, 7377-7383.
Tiscornia, G., Singer, O. and Verma, I. M. (2006). Production and purification of lentiviral vectors. *Nat. Protoc.* **1**, 241-245.
Tylzanowski, P., Mebis, L. and Luyten, F. P. (2006). The Noggin null mouse phenotype is strain dependent and haploinsufficiency leads to skeletal defects. *Dev. Dyn.* **235**, 1599-1607.
Wenger, R. H., Stiehl, D. P. and Camenisch, G. (2005). Integration of oxygen signaling at the consensus HRE. *Sci. STKE* **306**, re12.
Yun, Z., Maecker, H. L., Johnson, R. S. and Giaccia, A. J. (2002). Inhibition of PPAR gamma 2 gene expression by the HIF-1-regulated gene DEC1/Stra13: a mechanism for regulation of adipogenesis by hypoxia. *Dev. Cell* **2**, 331-341.